

Quantitative Analysis of Proxy Tasks for Anomalous Sound Detection

Seunghyeon Shin, Seokjin Lee (*Member, IEEE*)

Abstract—Anomalous sound detection (ASD) typically involves self-supervised proxy tasks to learn feature representations from normal sound data, owing to the scarcity of anomalous samples. In ASD research, proxy tasks such as AutoEncoders operate under the explicit assumption that models trained on normal data will increase the reconstruction errors related to anomalies. A natural extension suggests that improved proxy task performance should improve ASD capability; however, this relationship has received little systematic attention. This study addresses this research gap by quantitatively analyzing the relationship between proxy task metrics and ASD performance across five configurations, namely, AutoEncoders, classification, source separation, contrastive learning, and pre-trained models. We evaluate the learned representations using linear probe (linear separability) and Mahalanobis distance (distributional compactness). Our experiments reveal that strong proxy performance does not necessarily improve anomalous sound detection performance. Specifically, classification tasks experience performance saturation owing to insufficient task difficulty, whereas contrastive learning fails to learn meaningful features owing to limited data diversity. Notably, source separation is the only task demonstrating a strong positive correlation, such that improved separation consistently improves anomaly detection. Based on these findings, we highlight the critical importance of task difficulty and objective alignment. Finally, we propose a three-stage alignment verification protocol to guide the design of highly effective proxy tasks for ASD systems.

Index Terms—Anomalous Sound Detection, Proxy Tasks, Representation Learning, Self-supervised Learning, Task Alignment

I. INTRODUCTION

A COUSTIC-BASED condition monitoring has been adopted across various domains as microphone sensors are cost-effective and can operate in non-contact, occluded, or unlit environments. Acoustic monitoring can be categorized into two main streams, namely, sound event detection (SED) for surveillance [1], [2] and anomalous sound detection (ASD) for monitoring the continuous operating noise generated from machinery [3], [4]. Systems used for ASD are typically trained using only normal operating sounds, addressing the scarcity of anomalous data and the challenges associated with detecting unseen anomalous states [5]. Therefore, the system learns the distribution of normal sounds and determines an anomalous state by quantifying the deviation of the input signal from the normal distribution to detect anomalies using only normal data [6].

Neural networks must be trained exclusively on normal state audio; therefore the ultimate objective of detecting anomalies cannot be learned directly through supervised approaches.

This paper was produced by the IEEE Publication Technology Group. They are in Piscataway, NJ.

Manuscript received April 19, 2021; revised August 16, 2021.

This work has been submitted to the IEEE for possible publication. Copyright may be transferred without notice, after which this version may no longer be accessible.

This fundamental constraint necessitates the use of proxy task-auxiliary objectives that can be optimized using only normal data while implicitly learning representations useful for distinguishing anomalies. Consequently, proxy tasks are employed to indirectly learn representations to detect anomalies. Contemporary ASD research employs diverse proxy tasks. These include AutoEncoders (AE) that learn to reconstruct input signals [7], classification that leverages machine IDs or operating conditions [8], contrastive learning that acquires augmentation-invariant representations [9], source separation that isolates target sounds from mixtures [10], and transfer learning that employs pre-trained models [11]. These methods operate on distinct learning principles, namely, reconstruction, discrimination, and invariance learning; however, these principles share a common goal of capturing normal sound characteristics.

Despite this methodological diversity, the relationship between proxy task performance and ASD capability has received limited attention. For example, in the case of the widely adopted AE approach, the premise that anomalies increase reconstruction errors is consistently stated [12]; however, the extended hypothesis that optimizing reconstruction quality improves detection performance remains empirically unverified. Similarly, whether tight feature clustering from metric learning (e.g., ArcFace [13]) improves anomaly detection has not been tested. Moreover, researchers have observed that pretext task performance does not always predict downstream success in computer vision [14]. Whether similar patterns apply to ASD has yet to be systematically examined.

Understanding this relationship carries significant practical implications. Specifically, if proxy task optimization fails to improve ASD, then the common practice of designing and tuning proxy tasks based solely on their intrinsic metrics may be fundamentally misguided. Conversely, proxy metrics could serve as reliable surrogates for ASD performance during model development in the presence of strong correlations, reducing the reliance on anomalous samples in the validation phase.

The contributions of this study are as follows. First, we present the first systematic investigation into whether proxy task performance correlates with ASD capability. Although similar analyses exist in computer vision, the unsupervised detection objective and acoustic signal characteristics in ASD may yield distinct insights. Second, we propose a comprehensive evaluation framework, incorporating linear probe (LP), Mahalanobis distance (MD) [15], and proxy task metrics to assess learned representations from multiple perspectives. Third, we highlight the critical role of task difficulty and objective alignment and propose a three-stage verification protocol to effectively design proxy tasks.

The remainder of this paper is organized as follows. Sec-

tion II reviews the existing literature on ASD and on task alignment. Section III describes the proxy tasks employed herein and their experimental configurations. Section IV details the evaluation protocols used for proxy tasks and anomaly detection performance. Section V presents the experimental results with a preliminary analysis. Section VI discusses the relationship between proxy tasks and ASD performance in-depth. Finally, Section VII concludes the study and summarizes the limitations and directions for future research.

II. RELATED WORKS

A. General Unsupervised Anomalous Sound Detection

In the early stages, acoustic monitoring was primarily employed in surveillance applications to detect specific sound events such as gunshots, screams, or car crashes [1], [16], [17]. In these scenarios, collecting anomalous samples is relatively straightforward. In contrast, condition monitoring, to detect deviations from a normal state, was previously limited to specialized tasks such as heart sound detection [18] or monitoring specific machinery [19], [20] due to the difficulty in acquiring anomalous data.

However, the release of public datasets such as ToyADMOS [21] and MIMII [22], and the establishment of the Detection and Classification of Acoustic Scenes and Events (DCASE) challenges [5], have considerably increased the volume of research in this field. These datasets typically comprise normal operating sounds for training, whereas anomalous sounds, often recorded by intentionally damaging the machinery, are provided strictly for performance evaluation. To facilitate the development of highly robust systems suitable for real-world applications, ToyADMOS2 [23] was subsequently released to evaluate performance under domain shifts. A key design characteristic of these public datasets is the provision of several normal operating sounds for training, enforcing an unsupervised learning paradigm in which anomalous samples are reserved exclusively for the testing phase.

B. Proxy Tasks for Unsupervised Anomalous Sound Detection

In ASD environments restricted to normal operating sounds, direct training for anomaly detection is infeasible. Researchers employ various proxy tasks such that neural networks can learn the inherent characteristics of normal data, ultimately yielding features that distinguish anomalous inputs from learned normal patterns.

Reconstruction-based methods, particularly AEs, have been widely adopted since the establishment of the DCASE challenge baseline [24]. These methods assume that models trained on normal data will produce increased reconstruction errors for anomalies [25], [26]. Source separation-based approaches train neural networks to isolate target machine sounds from mixtures containing interfering noise. Recent studies on source separation-based ASD have demonstrated that separation models trained on normal sounds can be leveraged to detect anomalies [10], [27]. Discriminative approaches leverage auxiliary information such as machine IDs and operating conditions [28]. Recent studies on metric learning for ASD have demonstrated that metric learning objectives such as

ArcFace [13] enhance feature compactness, thereby improving detection performance [29]. Self-supervised methods, including contrastive learning frameworks such as SimCLR [30] and SimSiam [31], aim to learn augmentation-invariant representations [9], [32]. Conversely, transfer learning approaches employ models pre-trained on large-scale datasets. Specifically, models such as BEATs [33] and EAT [34] have demonstrated strong performances as feature extractors in recent ASD studies [35], [36]. These proxy tasks operate on explicit assumptions; however, the quantitative relationship between proxy task optimization and ASD performance has not been systematically investigated. Section III details the implementation and experimental design to examine this relationship across five proxy task families.

C. Evaluating Representations in Unsupervised Learning

Representations learned by neural networks are high-dimensional; therefore, directly evaluating their quality for ASD is inherently difficult. Consequently, indirect evaluation methods are employed to compare these representations, broadly categorized into qualitative and quantitative approaches.

Qualitative evaluation is typically conducted using visualization techniques based on dimensionality reduction, such as t-SNE [37] or UMAP [38]. These methods project the high-dimensional feature space onto a low dimensional plane, allowing the clustering of compact data points of the same class and the separation from other classes to be visually inspected. Although these visualizations offer intuitive insights, they are sensitive to hyperparameter settings and do not yield numerical metrics, complicating the direct quantitative comparisons between different systems.

Quantitative evaluation involves attaching an auxiliary module to the learned representations to derive numerical metrics. The most widely adopted approach is the LP [39], which assesses the quality of features by training a single linear classifier on top of the fixed (frozen) output features of the pre-trained network, utilizing a labeled evaluation dataset. The resulting performance indicates the ease with which the representations can be separated by a linear decision boundary.

Although high linear separability is generally indicative of a well-trained network, the quality of a representation does not necessarily guarantee linear separability [40]. Learned representations are often evaluated using alignment and uniformity metrics in the domain of unsupervised learning, particularly contrastive learning [41]. Alignment measures the proximity of features from augmented views of the same sample, whereas uniformity assesses the even distribution of features from different samples. However, these metrics are intrinsically designed for frameworks that depend heavily on data augmentation. Consequently, they are ill-suited for evaluating other proxy tasks, such as those based on reconstruction-based objectives (e.g., AE and source separation), in which such augmentation strategies are not central to the learning process.

D. Proxy-Target Alignment in Other Domains

The relationship between proxy (or pretext) and downstream task performances has been investigated in the domain of

machine learning, particularly in computer vision. A large-scale evaluation [42] of 13 self-supervised models across 40 downstream tasks revealed that the accuracy of ImageNet Top-1 correlates well with many-shot recognition but poorly with few-shot learning, object detection, and dense prediction tasks. This study demonstrated that high pretext task performance does not universally guarantee downstream success. Similarly, research addressing the specificity of proxy tasks has demonstrated that features optimized for pretext tasks may become overly specialized, limiting the generalization of these features to target tasks [14]. These findings from the domain of computer vision suggest that the assumed link between proxy and target task performance warrants careful examination. In the ASD domain, however, such systematic analysis has not been conducted. Although the foundational assumption of reconstruction-based methods, i.e., anomalies increase reconstruction errors, is explicitly stated in DCASE baseline system descriptions [5], the extended hypothesis, i.e., optimizing reconstruction quality improves ASD performance, has not been empirically tested. This study addresses this research gap via a systematic empirical analysis across five proxy task families.

III. PROXY TASKS AND CONFIGURATIONS

A. Overview

To systematically investigate the relationship between proxy task performance and ASD capability, we selected five proxy task families that represent the diverse learning paradigms currently dominant in ASD research. These tasks and their configurations are comprehensively summarized in Table I. First, we employ AE and source separation, representing the reconstruction-based paradigm. These methods rely on the hypothesis that models trained on normal data will yield large errors or degrade outputs when processing anomalies, thereby manifesting distinguishable differences in the feature space. Second, we employ classification tasks that leverage auxiliary attribute information, such as machine IDs, for the discriminative paradigm. Recent approaches in this domain frequently incorporate metric learning objectives, such as ArcFace [13], to enforce compact intra-class clustering and enhance decision boundaries. Third, we adopt contrastive learning frameworks, specifically SimCLR [30] and SimSiam [31], representing the self-supervised paradigm. These methods focus on learning invariant representations by maximizing agreement between augmented views of the same sample, essential for evaluating feature robustness in the absence of explicit labels. Finally, to address the transfer learning paradigm, we evaluate pre-trained models. We employ representations from large-scale foundational models to assess the transferability of general acoustic features to the specific domain of ASD.

To ensure an effective comparison, we use consistent training configurations. All neural networks are trained using the AdamW optimizer [43], coupled with a StepLR scheduler for 200 epochs. We select models based on the lowest training loss rather than employing a separate validation set to maximize the use of limited training data for learning ASD-suitable representations and strictly prevent information leakage from

anomalous samples during the validation phase. Unless otherwise noted in the respective subsections, input signals are processed as 10-s audio clips (16 kHz) converted to log-mel spectrograms with 128 mel bins, using an FFT size of 1024 and a hop size of 512.

B. AutoEncoder

AEs have served as the foundational baseline for the DCASE Challenge Task 2 [24] series since 2020, establishing the standard benchmark for unsupervised ASD. Including AEs is, therefore, essential to provide a reference point for performance comparison in our analysis. Although simple, reconstruction-based methods remain effective, relying on the premise that models trained to minimize reconstruction error on normal data will increase errors under anomalous inputs that deviate from the learned distribution. The underlying hypothesis is that improved reconstruction of normal patterns should clarify the separation from anomalies, thereby improving ASD performance.

The fundamental objective of an AE is to learn a compressed representation of the input signal and subsequently reconstruct the original signal from this latent code. During training, the network optimizes its parameters to minimize the discrepancy between the input and the reconstructed output. We adopt a dense AE architecture consistent with the DCASE 2022 Task 2 baseline [24]. The encoder and decoder each consist of five fully connected layers. The input is a 640-dimensional vector formed by concatenating five consecutive frames of a 128-bin log-mel spectrogram. Moreover, the encoder progressively compresses this input through hidden layers to a bottleneck latent space, and the decoder reconstructs the original representation from this latent code. This bottleneck constraint compels the network to prioritize the dominant patterns of the normal training sound distribution, thereby inhibiting the accurate reconstruction of unseen irregular patterns.

Unlike typical representation learning, which employs the latent vector, reconstruction-based ASD employs the reconstruction error as the feature representation, following the DCASE baseline system configuration. We use the element-wise reconstruction error vector, which captures per-bin discrepancies between the input and output spectrograms, directly reflecting the inability of the model to reconstruct anomalous time-frequency patterns.

To systematically analyze the effect of model capacity on the proxy-ASD relationship, we vary the hidden layer (64, 128, 256) and bottleneck (4, 8, 16) dimensions, yielding nine experimental configurations with different compression ratios.

C. Classification

Classification is a dominant proxy task in the ASD domain. Prior studies have demonstrated that incorporating granular attribute information, such as operation speeds, machine loads, or domain labels, can enhance detection performance [28], [29]. However, in this study, we restrict the scope to standard machine ID classification, excluding detailed attribute metadata, to evaluate the fundamental discriminative capability

TABLE I

OVERVIEW OF THE PROXY TASKS AND EXPERIMENTAL CONFIGURATIONS USED IN THIS STUDY. THE ‘FEATURE FOR ASD’ COLUMN SPECIFIES THE REPRESENTATION EXTRACTED FOR ANOMALY DETECTION.

Learning paradigm	Proxy task	Input data	Learning objective (loss)	Feature for ASD (output)
Reconstruction	AE	Log-mel Spectrogram	Mean Absolute Error	Element-wise reconstruction error
	Source separation	Mixture Spectrogram	SI-SDR (signal separation)	Concatenated channel-pooled features
Discriminative	Classification	Log-mel spectrogram	Cross-entropy / ArcFace	Backbone output (penultimate layer)
Self-supervised	Contrastive learning (SimCLR, SimSiam)	Augmented views	NT-Xent (SimCLR) Neg. Cosine Sim. (SimSiam)	Backbone output (ResNet)
Transfer learning	Pre-trained models	Raw waveform	(Pre-trained on AudioSet)	Mean-pooled embeddings

derived solely from acoustic signals and to ensure a generalizable assessment across different deployment scenarios. The hypothesis is that tight intra-class clustering in the feature space should yield highly discriminative representations for anomaly detection.

We employ two representative training objectives. The first is the standard cross-entropy loss, which trains the network to classify inputs by maximizing the predicted probability of the ground-truth class. The second is ArcFace (additive angular margin loss) [13], a metric learning objective that imposes an additive angular margin penalty. This explicitly enforces intraclass compactness within the feature space, which is expected to improve the distinguishing of anomalies from normal patterns.

We employ the ResNet family (ResNet-18, 34, 50, 101, and 152) [44], a standard choice for extracting deep acoustic representations, for the backbone architecture. The structural difference between the two objectives is related to the auxiliary head attached to the backbone. Specifically, CE uses standard features for linear layer mapping to class logits, whereas ArcFace employs a margin-based projection layer to compute angular distances. These auxiliary heads are used exclusively during proxy task training. For ASD evaluation, we discard these heads and employ the feature vector from the penultimate layer (the ResNet backbone output) as the representation, yielding feature dimensions of 512 for ResNet-18/34, and 2048 for ResNet-50/101/152. The combination of five backbone variants and two loss functions yields ten experimental configurations, enabling the effects of network capacity and training objective on the proxy-ASD relationship to be analyzed.

D. Source Separation

Source separation represents a distinct paradigm in unsupervised ASD, diverging from standard compression or discrimination approaches. Preliminary studies have investigated the utility of source separation for ASD; however, the quantitative relationship between separation quality and detection performance has not yet been systematically analyzed [27], [45]. We include this task herein to investigate whether the objective of isolating target sounds, distinct from reconstruction or classification, yields representations beneficial for ASD. We posit that improved separation capability correlates with a highly precise characterization of normal sound patterns, thereby enhancing the detection of deviations.

The core objective is to estimate the target machine’s clean signal from a synthetic mixture. During training, the model receives a mixture of the target normal sound and randomly sampled auxiliary noise at varying signal-to-noise ratios (-5–5 dB). By learning to filter out these variable noise components, the network implicitly captures the inherent structural patterns of normal sounds required to accurately reconstruct signals.

We adopt the architecture proposed in our previous work [27], based on the CMGAN framework [46]. This architecture features a Dilated DenseNet-based encoder and decoder, with conformer [47] blocks interposed between them to enhance temporal modeling. Unlike the AE, which directly employ the reconstruction error, we leverage the intermediate representations learned by the separation network. Specifically, we extract feature maps from the output of the dense encoder and each subsequent conformer block; for a model with N conformer blocks, features are aggregated from $N + 1$ extraction points. Due to the computational complexity of processing full 10-s sequences, the network operates on 2-s segments. Channel-wise average pooling is applied to each extraction point, and the final representation is obtained by concatenating these pooled vectors along the time axis, capturing multi-scale structural characteristics. To analyze the relation of separation capability with ASD performance, we vary the number of conformer blocks (0, 1, 2, 4) and the channel width (64, 128), yielding eight experimental configurations.

E. Contrastive Learning

Contrastive learning is a widely adopted self-supervised methodology that leverages data augmentation to learn representations without explicit labels. We include this task to systematically investigate whether augmentation-invariant representations benefit anomaly detection. The hypothesis is that learning to capture intrinsic acoustic patterns invariant to augmentation may distinguish normal sounds from anomalies.

The fundamental objective is to learn consistent representations from the same input regardless of applied augmentations. To generate augmented views, we apply a combination of time-domain masking, frequency-domain masking, pitch shifting, time stretching, and white noise injection. These augmentations are selected to cover both spectral and temporal variations commonly encountered in acoustic signals. We employ two representative frameworks. SimCLR [30] maximizes the similarity between positive pairs (augmented views from

the same sample) while minimizing the similarity between negative pairs (views from different samples), using NT-Xent loss. In contrast, SimSiam [31] relies solely on positive pairs without requiring negative samples.

For the backbone architecture, we employ the ResNet family (ResNet-18, 34, 50, 101, and 152) [44]. An MLP projection head is attached to the backbone during training, consisting of two hidden layers (Linear–BatchNorm–ReLU) followed by a final linear layer that projects features into a 128-dimensional space where the contrastive objective is applied. This projection head is discarded for ASD evaluation; the feature representation is extracted from the backbone output (penultimate layer), yielding 512-dimensional vectors for ResNet-18/34 and 2048-dimensional vectors for ResNet-50/101/152. The combination of five backbone variants and two contrastive frameworks yields ten experimental configurations, enabling analysis of the effect of model capacity and learning strategy on the proxy-ASD relationship.

F. Pre-trained Models

Pre-trained models have demonstrated strong performances in recent ASD studies, serving as feature extractors or teacher models for knowledge distillation. We include this paradigm to examine whether general audio understanding, as measured by AudioSet [48] classification performance, transfers effectively to ASD. The implicit assumption in adopting pre-trained models is that increased classification accuracy on large-scale audio datasets should yield increased discriminative representations for anomaly detection. Unlike other proxy tasks trained from scratch, we evaluate off-the-shelf models without additional fine-tuning on the target dataset. This allows us to assess the intrinsic transferability of pre-trained representations to the ASD domain.

We selected two representative model families widely adopted in ASD research. These include BEATs [33], which employs iterative audio pre-training with acoustic tokenizers, and EAT [34], which employs masked audio modeling. Both models are pre-trained and evaluated on the AudioSet dataset, with mean average precision (mAP) serving as the common benchmark for general audio classification capability.

We employ mean pooling over the time axis of the model outputs for feature extraction, yielding 768-dimensional vectors for BEATs and EAT-base, and 1536-dimensional vectors for EAT-large. We evaluate four model variants, namely, BEATs-iter3, BEATs-iter3+ (additionally fine-tuned on AS-2M), EAT-base, and EAT-large. We select these four variants as they represent two distinct pre-training approaches widely adopted in recent ASD research, with publicly reported mAP scores enabling direct comparison of proxy task performance.

IV. EVALUATION METHODOLOGY

A. Evaluation Protocol

To evaluate the representations consistently learned by feature extractor F , we employ a unified evaluation protocol. Assessing these representations involves two essential steps as follows: deriving an anomaly score from the extracted feature

vectors and quantitatively evaluating the overall detection performance of the system based on these calculated scores.

We adopt simple scoring mechanisms that avoid intricate post-processing or reliance on auxiliary information to ensure that the evaluation focuses precisely on the quality of the learned representations, rather than on the complexity of the scoring backend. We employ two distinct, complementary scoring protocols for feature evaluation: LP, which utilizes a single linear classifier to assess the linear separability of the representations, and MD [15], which evaluates the distributional compactness of the normal features. We quantify the final anomalous sound detection performance using the area under the receiver operating characteristic curve (AUC). The AUC is widely adopted in ASD research as it provides a robust, threshold-independent measure of the system's ability to distinguish between normal and anomalous samples.

For the evaluation, we employed the ToyADMS2 [23] and MIMII [22] datasets, adopting the experimental configuration of the DCASE 2022 Challenge Task 2 (Fig. 1). In this context, a "section" is defined as a subset of the dataset dedicated to a specific type of domain shift. Each section represents one of four domain shift scenarios, i.e., differences in machine physical parameters, environmental conditions, post-maintenance characteristics, or recording devices. Accordingly, we define two evaluation scenarios based on the relationship between training and test domains. Specifically, in-domain evaluation assesses generalization to unseen samples within the same section, whereas out-domain evaluation measures robustness against domain shifts by testing on entirely different sections not encountered during training. For each of the seven machine types covered in the experiment, the training set comprises 6,000 normal samples collected from six sections (1,000 samples per section). The evaluation set consists of 600 samples from three sections, comprising 100 normal and anomalous samples each per section.

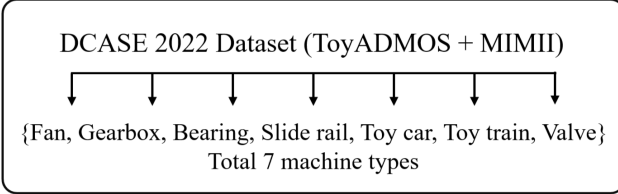
To quantitatively analyze the correlation between proxy task performance and ASD performance, we employ the non-parametric Spearman's rank correlation coefficient. Given the limited sample size, p -values were computed using an exact test to ensure statistical validity.

B. Anomaly Score Calculation

1) *Linear Probe*: LP is a widely adopted technique to evaluate representation quality by measuring the linear separability of features extracted from a trained network. In this protocol, a single linear layer is appended to the pre-trained feature extractor, the weights of which remain frozen. This linear layer is subsequently trained to perform a binary classification task, distinguishing between normal and anomalous states. For input acoustic signal x , feature representation h is extracted as defined in Section III. Consequently, h corresponds to the reconstruction error of the AE, the penultimate layer output for classification and contrastive learning, or the concatenated features for source separation. Formally, we define the feature vector as $h = F(x)$. Subsequently, this vector is passed through the linear classifier to yield logits z , as defined below.

$$z = Wh + b, \quad (1)$$

(a) Overall Structure



(b) Per-Machine Data Split

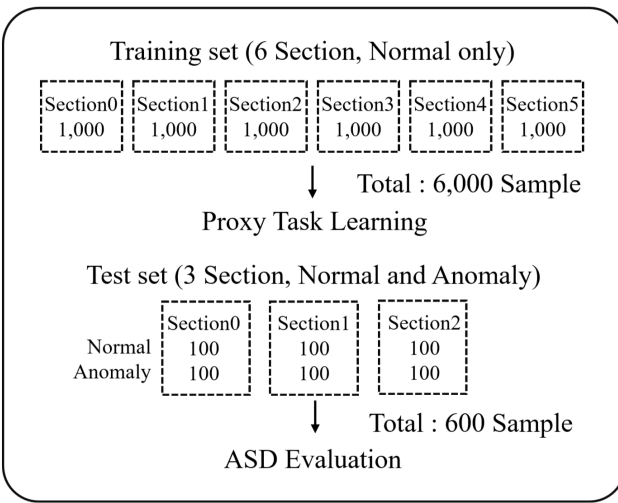


Fig. 1. Dataset configuration of the DCASE 2022 challenge. (a) Overall structure comprising seven machine types. (b) Per-machine data split: training set (six sections, 6,000 normal samples) for proxy task learning and test set (three sections, 600 total: 300 normal + 300 anomaly) for ASD evaluation. The configuration is identical across all machines.

where \mathbf{W} and \mathbf{b} denote the weight matrix and the bias vector of the linear layer, respectively. These parameters are updated during the classifier training phase. Training is conducted using a subset of the evaluation data containing both normal and anomalous samples, to minimize the cross-entropy loss function defined as

$$\mathcal{L}_{ce} = - \sum_{c=0}^1 y_c \log(p_c), \quad (2)$$

where y_c denotes the ground-truth label for class c (normal or anomalous) and p_c represents the probability of class c , obtained by applying the softmax function to the logit vector \mathbf{z} .

$$p_c = \frac{\exp(z_c)}{\sum_{i=0}^1 \exp(z_i)}. \quad (3)$$

Once the training is complete, the anomaly score for a test sample x is defined as the softmax probability corresponding to the anomalous class ($c = 1$).

$$S_{LP}(x) = p_1 = \frac{\exp(z_1)}{\exp(z_0) + \exp(z_1)}. \quad (4)$$

Herein, we construct two distinct data configurations for the LP evaluation to assess performance under different conditions. Specifically, the first configuration, termed the *in-domain LP*, measures generalization performance on unseen

data within the same domain. The data are split equally in each section, with 300 samples used for training and the remaining 300 samples for evaluation. The second configuration, termed the *out-domain LP*, evaluates robustness against domain shifts. This setup adopts a leave-one-out cross-validation approach, i.e., the model is trained on 400 samples from two source sections and evaluated on 200 samples from the remaining unseen target section. This process is repeated for all three sections.

2) *Mahalanobis Distance*: Unlike LP, which requires a labeled subset of the evaluation data, the MD is a non-parametric method that relies solely on the statistical distribution of the normal training data. MD, owing to its computational simplicity and effectiveness, is widely adopted in anomaly detection and out-of-distribution detection tasks.

To calculate MD, we first compute mean vector μ_{normal} and covariance matrix Σ_{normal} from feature vectors $\mathbf{h} = F(x)$ of all normal training samples. During the evaluation phase, anomaly score S_{MD} for a test input x_{test} with feature vector \mathbf{h}_{test} is calculated as the MD with respect to the learned normal distribution.

$$S_{MD}(x_{\text{test}}) = (\mathbf{h}_{\text{test}} - \mu_{\text{normal}})^T \times \Sigma_{\text{normal}}^{-1} (\mathbf{h}_{\text{test}} - \mu_{\text{normal}}), \quad (5)$$

where $(\cdot)^T$ denotes the transpose operation and $\Sigma_{\text{normal}}^{-1}$ represents the inverse of the covariance matrix. Although computing domain-specific statistics can enhance detection performance, the primary objective of this study is to evaluate the intrinsic quality of the representations without relying on auxiliary information. Therefore, we refrain from using domain labels and instead compute a single set of global statistics from the entire normal training dataset for the evaluation.

C. Method Used to Evaluate Proxy Tasks

This study primarily aims to verify whether performance improvements in proxy tasks effectively translate to the acquisition of representations suitable for ASD. For this, we evaluate the extent to which each neural network has learned its designed proxy task using standard performance metrics. The scope of this evaluation encompasses AE, classification, source separation, contrastive learning, and representations from pre-trained models. Specifically for pre-trained models, as we use off-the-shelf models trained for AudioSet classification, and we adopt the mAP reported in the original study as the proxy task performance metric.

1) *AutoEncoder*: The objective of an AE is to compress an input signal into a latent representation and subsequently reconstruct the original signal. In the context of ASD, the AE is expected to yield considerably higher reconstruction errors for anomalous than those for normal data, as the distribution of anomalies differs from that of the normal training data.

Herein, we employ log-mel spectrograms as both input and output. The reconstruction quality was determined based on the MAE. The MAE represents the L1 distance between the original and reconstructed spectrograms, normalized by

the total number of time-frequency bins (N), which can be interpreted as the average error in decibels (dB).

$$\mathcal{L}_{\text{MAE}} = \frac{1}{N} \sum_{i=1}^N \left| M_{\text{in}}^{(i)} - M_{\text{out}}^{(i)} \right|, \quad (6)$$

where N denotes the total number of time-frequency bins, and $M_{\text{in}}^{(i)}$ and $M_{\text{out}}^{(i)}$ represent the i -th bin of the input and output mel-spectrograms, respectively.

2) *Classification*: The classification-based proxy task trained the neural network to distinguish between distinct classes, such as specific machine IDs or operating conditions defined in the dataset. To evaluate classification performance, we employ the Macro F_1 -score, calculated as the arithmetic mean of the class-wise F_1 -scores. The F_1 -score is defined as the harmonic mean of precision and recall:

$$F_1 = 2 \cdot \frac{\text{Precision} \cdot \text{Recall}}{\text{Precision} + \text{Recall}}. \quad (7)$$

When the network is trained using cross-entropy loss, the final output represents class probabilities, allowing for the direct derivation of classification metrics. However, metric learning approaches that operate in the feature space, such as angular margin loss (e.g., ArcFace), do not inherently produce probability outputs suitable for immediate classification scoring. Therefore, to evaluate the classification performance of models trained using angular margin loss, we attach a single linear classifier to the pre-trained feature extractor. With the weights of the backbone network frozen, we train only this auxiliary linear layer to predict class labels and compute the F_1 -score.

3) *Source Separation*: The objective of the source separation task is to isolate target acoustic signal x_{target} from mixture signal x_{mix} . To evaluate separation performance, we generate evaluation mixtures by combining signals from the target class with interfering signals from non-target classes. We construct evaluation sets with signal-to-noise ratios of -5 , 0 , and 5 dB, generating 1,000 samples for each condition. The performance is assessed using the improvement in scale-invariant signal-to-distortion ratio (SI-SDRi) [49]. The SI-SDR is defined as follows:

$$\text{SI-SDR} = 10 \log_{10} \left(\frac{\|ax_{\text{target}}\|_2^2}{\|ax_{\text{target}} - \hat{x}_{\text{target}}\|_2^2} \right), \quad (8)$$

where a denotes the optimal scaling factor that minimizes the L2 error between the target and estimated signal and \hat{x}_{target} represents the signal estimated by the neural network.

4) *Contrastive learning*: Contrastive learning aims to acquire representations by minimizing the distance between positive pairs (augmented views of the same sample) while maximizing the distance between negative pairs (views of different samples). To assess the quality of the learned feature space, we adopt the alignment and uniformity metrics proposed in [41]. Alignment quantifies the closeness of feature representations for positive pairs derived from the same original sample.

$$\mathcal{L}_{\text{align}}(f; \alpha) = \mathbb{E}_{(x, y) \sim P_{\text{pos}}} [\|f(x) - f(y)\|_2^\alpha], \quad \alpha > 0, \quad (9)$$

TABLE II
COMPARISON OF THE PROXY TASK AND ASD PERFORMANCES BASED ON AE CONFIGURATION.

Model config (latent, hidden)	Test MAE(\downarrow) ($\times 10^{-3}$)	Linear probe (AUC %)		Mahalanobis(\uparrow) (AUC%)
		In-domain(\uparrow)	Out-domain(\uparrow)	
4, 64	4.59	71.68	63.56	56.11
4, 128	4.46	70.52	64.99	56.51
4, 256	4.40	71.88	63.15	57.38
8, 64	4.46	69.84	62.51	55.52
8, 128	4.34	70.43	64.31	56.97
8, 256	4.25	71.92	63.95	57.30
16, 64	4.41	70.68	62.17	55.74
16, 128	4.26	71.18	63.25	56.55
16, 256	4.13	72.45	63.24	57.65

where $f(x)$ denotes the L_2 -normalized feature vector ($f(x) = F(x)/\|F(x)\|_2$) mapped to the unit hypersphere, and P_{pos} denotes the distribution of positive pairs. Uniformity measures the uniformly with which the feature vectors are distributed across the hypersphere, ensuring that the representations preserve maximal information.

$$\mathcal{L}_{\text{uniformity}}(f; t) = \log \mathbb{E}_{x, y \stackrel{\text{i.i.d.}}{\sim} P_{\text{data}}} [\exp(-t\|f(x) - f(y)\|_2^2)], \quad t > 0, \quad (10)$$

where t is a scaling parameter and x, y are independently sampled from data distribution P_{data} .

V. EXPERIMENTAL RESULTS

A. AutoEncoder results

Table II summarizes the results across nine configurations. The experimental results suggest that improvements in the proxy task (AE reconstruction) do not consistently improve ASD performance.

First, for the in-domain LP, we observed a weak trend, i.e., performance improved as the hidden dimension increased; however, notable exceptions were present. For instance, although the (16, 256) configuration achieved both the lowest MAE (4.13×10^{-3}) and the highest AUC (72.45%), the (4, 256) configuration achieved the second-highest AUC (71.88%) despite having a higher reconstruction error (4.40×10^{-3}) than three other configurations. This indicates that a better AE model (lower MAE) does not necessarily yield representations with superior linear separability for ASD.

Second, no clear correlation was observed in the out-domain LP results. Both the best- (16, 256) and worst-performing configurations (4, 64) yielded suboptimal ASD performance within the overall results. Furthermore, the performance deviation across models was minimal, suggesting a limited connection between AE reconstruction capability and domain-robust ASD performance.

Finally, during the MD evaluation, we observe that increasing the hidden dimension consistently improve ASD performance within groups sharing the same latent dimension. However, this trend does not apply across configurations with different latent dimensions, revealing little connection to the overall AE reconstruction performance.

TABLE III

COMPARISON OF THE PROXY TASK AND ASD PERFORMANCES BASED ON CLASSIFICATION NETWORK CONFIGURATION AND LOSS FUNCTION.

Model config (backbone)	F_1 -Score(↑) (%)	Linear probe (AUC%)		Mahalanobis(↑)
		In-domain(↑)	Out-domain(↑)	(AUC%)
Loss function: ArcFace				
ResNet-18	98.43	64.32	57.69	53.90
ResNet-34	98.50	59.27	56.48	54.48
ResNet-50	97.93	62.86	55.68	53.23
ResNet-101	97.87	62.33	56.53	54.92
ResNet-152	97.95	63.14	58.60	54.27
Loss function: Cross-Entropy				
ResNet-18	98.62	71.20	60.69	58.16
ResNet-34	98.66	64.80	59.14	58.61
ResNet-50	97.43	65.92	56.42	57.00
ResNet-101	98.36	67.78	59.45	59.59
ResNet-152	97.40	66.14	59.80	61.21

B. Classification Result

Table III lists the results across ten configurations. The experimental results indicate that performance on the classification task saturated, achieving F_1 -scores exceeding 97% across all configurations, regardless of the model architecture or training objective. This suggests that the classification problem defined by the current dataset configuration is relatively trivial. Consequently, the performance metrics of the proxy task lacked the discriminative power to explain correlations with ASD performance.

However, despite the comparable performance in the proxy task, considerable deviations in ASD performance were observed depending on the loss function and model architecture. First, cross-entropy-based models generally outperformed ArcFace-based models in ASD tasks in terms of the loss function. This finding contradicts those reported in some prior studies, suggesting that the full effectiveness of ArcFace may depend on the active utilization of granular attribute information. ArcFace is designed to maximize angular margins between classes, which may be less effective when class boundaries (machine IDs) do not directly correspond to the normal/anomaly distinction targeted in ASD.

Furthermore, distinct characteristics were observed even within the cross-entropy-based models, depending on the architecture. The smallest model, ResNet-18, exhibited the highest linear separability in both in-domain and out-domain LP tests. In contrast, the largest model, ResNet-152, achieved the best distributional compactness during MD evaluation.

C. Source Separation Results

Table IV lists the results across eight configurations. The experimental results demonstrated a distinct positive correlation between the separation (SI-SDRi) and ASD performances. As the complexity of the CMGAN model increased (owing to additional conformer blocks and channels), the SI-SDRi consistently improved from 2.29 dB to 3.92 dB. Notably, this improvement in the proxy task was accompanied by consistent performance gains across all the ASD evaluation metrics, including in-domain LP, out-domain LP, and MD.

This trend is particularly evident when comparing the performance extremes. The lowest-performing model (0-block,

TABLE IV

COMPARISON OF THE PROXY TASK AND ASD PERFORMANCES BASED ON THE NETWORK CONFIGURATION OF THE SOURCE SEPARATION.

Model config (Conformer block, Channel)	SI-SDRi(↑) (dB)	Linear probe (AUC%)		Mahalanobis(↑)
		In-domain(↑)	Out-domain(↑)	(AUC%)
0-block, 64-ch	2.29	55.87	52.06	55.80
0-block, 128-ch	2.61	58.45	54.82	55.72
1-block, 64-ch	2.78	61.38	54.68	56.88
1-block, 128-ch	3.40	65.07	59.83	60.51
2-block, 64-ch	3.03	62.61	57.14	58.56
2-block, 128-ch	3.57	66.02	62.17	59.24
4-block, 64-ch	3.24	62.49	60.32	58.82
4-block, 128-ch	3.92	68.35	64.09	61.22

TABLE V

COMPARISON OF THE PROXY TASK AND ASD PERFORMANCES BASED ON THE NETWORK CONFIGURATION OF CONTRASTIVE LEARNING AND THE LOSS FUNCTION.

Model config (Backbone)	Alignment (↓)	Uniformity (↓)	Linear probe (AUC%)		Mahalanobis(↑)
			In-domain(↑)	Out-domain(↑)	(AUC %)
Loss function: SimCLR					
ResNet-18	0.24	-0.93	65.09	57.80	51.57
ResNet-34	0.24	-0.99	62.13	52.88	51.47
ResNet-50	0.13	-0.48	63.02	59.78	49.81
ResNet-101	0.17	-0.68	60.24	55.21	50.02
ResNet-152	0.17	-0.71	59.08	52.33	50.24
Loss function: SimSiam					
ResNet-18	0.31	-0.82	59.49	55.98	52.49
ResNet-34	0.20	-0.65	59.01	53.65	49.07
ResNet-50	0.09	-0.41	52.42	51.96	51.85
ResNet-101	0.07	-0.21	49.53	50.28	45.88
ResNet-152	0.04	-0.18	50.01	49.91	47.19

64-ch) yielded an out-domain LP score of 52.06%, comparable to random guessing, indicating a failure to learn meaningful representations for ASD. Conversely, the highest-performing separation model (4-block, 128-ch) achieved substantial improvements, showing gains of 12.48% and 12.03% in in-domain and out-domain LPs, respectively, and a 5.42% increase in MD performance relative to the baseline model.

D. Results Obtained from Unsupervised Contrastive Learning

Table V lists the results across ten configurations. The experimental results indicate that contrastive learning approaches generally failed to acquire meaningful representations, subsequently yielding poor ASD performance, using the current dataset. Notably, phenomena indicative of model collapse became increasingly pronounced as the model capacity increased. In the case of SimSiam, the smallest model, ResNet-18, recorded an alignment of 0.31 and uniformity of -0.82. However, as the model size increased to ResNet-152, the alignment reduced to 0.04, whereas uniformity increased sharply to -0.18. Although the reduction in the alignment score might initially seem favorable, the simultaneous increase in uniformity (approaching zero) suggests that the model has converged to a trivial solution, mapping all inputs to a narrowly confined region in the feature space. The performance of SimCLR exhibited a similar degradation trend. On comparing the results obtained from ResNet-152 to those obtained from ResNet-18, uniformity appeared to have considerably worsened, shifting from -0.93 to -0.71, whereas alignment decreased from 0.24 to 0.17, further suggesting feature collapse. This failure in proxy task training was reflected in the ASD performance. All

TABLE VI
COMPARISON OF THE PROXY TASK AND ASD PERFORMANCES BASED ON THE DIFFERENT PRE-TRAINED MODEL CONFIGURATIONS.

Model config	AS-2M(\uparrow)	Linear probe (AUC %)		Mahalanobis(\uparrow)
	mAP (%)	In-domain(\uparrow)	Out-domain(\uparrow)	(AUC%)
EAT-large	49.5	69.83	56.79	60.40
EAT-base	48.9	69.67	58.79	60.53
BEATs-iter3	48.0	71.41	58.71	62.29
BEATs-iter3+	48.6	73.73	62.35	63.71

experimental configurations yielded AUC scores comparable to random guessing in terms of the MD. Even in the LP evaluation, yielding relatively better results, the performance was limited to 65.09% for in-domain and 59.78% for out-domain scenarios.

E. Pre-trained Model Results

Table VI lists the results across four model variants. Contrary to expectations, the experimental results revealed an inconsistent relationship between general audio classification performance and ASD capabilities. Specifically, the BEATs-iter3+ model achieved the highest performance across all ASD evaluation metrics despite recording the second-lowest classification performance (48.6% mAP) among the four comparison models. A similar divergence was observed within the EAT models; the EAT-base model yielded a lower mAP (48.9%) than the EAT-large model (49.5%); however, the former outperformed the latter model in both out-domain LP and MD evaluations. These findings suggest that the acoustic features required for ASD may differ from those optimized for general audio classification problems. Furthermore, general-purpose pre-trained representations are assumed to be transferable to ASD; however, our results suggest that without task-specific fine-tuning, the intrinsic performance of these large-scale models was inefficient relative to their computational cost and parameter size.

VI. DISCUSSIONS

A. Correlation Between the Proxy Task and ASD Performances

In this section, we examine whether the intuitive hypothesis, i.e., better proxy task performance improves ASD capability, applies in practice. Table VII lists the Spearman correlation coefficients across all experimental configurations, and the scatter plots are presented in Figs. 2–4. Our analysis reveals that the proxy-ASD relationship varied substantially depending on task characteristics, consistent with findings obtained in computer vision field [42].

Source separation was the only proxy task demonstrating consistent positive correlation across all evaluation metrics ($\rho > 0.95$, $p < 0.01$). As SI-SDRi improved from 2.29 dB to 3.92 dB, all ASD metrics increased correspondingly, i.e., in-domain LP increased from 55.87% to 68.35%, out-domain LP from 52.06% to 64.09%, and MD from 55.80% to 61.22%. This consistent co-improvement suggests that learning to isolate normal sound patterns from interference directly benefits

TABLE VII
SPEARMAN CORRELATION COEFFICIENTS (ρ) BETWEEN THE PROXY TASK METRICS AND ASD PERFORMANCE. BOLD INDICATES STATISTICAL SIGNIFICANCE (* $p < 0.05$, ** $p < 0.01$, *** $p < 0.001$). FOR AE AND CONTRASTIVE LEARNING; NEGATIVE ρ INDICATES A POSITIVE RELATIONSHIP AS LOW METRIC VALUES REPRESENT HIGH PERFORMANCE.

Proxy task	In-domain LP	Out-domain LP	MD
AutoEncoder	−0.57	0.10	−0.78*
Classification (CE)	−0.30	0.20	−0.10
Classification (ArcFace)	−0.10	−0.30	−0.30
Source separation	0.98***	0.95**	0.95***
Contrastive (SimCLR)	−0.10	0.50	−0.90
Contrastive (SimSiam)	−0.90	−1.00*	−0.80
Pre-trained	−0.60	−0.40	−0.80

anomaly detection, representing an ideal case in which task difficulty and objective alignment are simultaneously satisfied.

The classification tasks revealed no significant correlation across any metric ($|\rho| \leq 0.3$, $p > 0.6$), attributable to performance saturation. All configurations achieved F_1 scores exceeding 97%, indicating that the task was trivially easy. This ceiling effect eliminated discriminative power in the proxy metric. However, notable differences in ASD performances emerged based on loss function and architecture, i.e., cross-entropy models outperformed ArcFace in LP evaluations, whereas the large models (ResNet-152) achieved better MD performance than the small ones (ResNet-18), despite comparable F_1 -scores.

Contrastive learning tasks failed to learn meaningful representations owing to apparent model collapse. SimSiam exhibited clear degradation as model capacity increased, i.e., uniformity worsened from −0.82 to −0.18, approaching the trivial solution. Although SimSiam showed significant correlation in out-domain LP ($\rho = −1.0$, $p = 0.016$), the absolute ASD performance remained poor (maximum 55.98%), and the MD results were comparable to random guessing. We attribute this failure to insufficient acoustic diversity in the dataset for effective contrastive learning.

The AE demonstrated metric-dependent correlation. No significant correlation was observed in LP evaluations; however a significant correlation emerged with MD ($\rho = −0.78$, $p = 0.018$). This suggests that the reconstruction objective aligns with distributional compactness but not with linear separability. Notably, despite the absence of LP correlation, the AE models maintained consistently high absolute performance (out-domain LP: 62.17–64.99%), indicating that reconstruction-based learning captures ASD-relevant features even when proxy improvements do not predict performance variants.

Pre-trained models revealed no significant correlation between AudioSet mAP and ASD performance. BEATs-iter3+ achieved the highest ASD scores across all metrics despite lower mAP than EAT-large, suggesting that general audio classification features do not directly transfer to anomaly detection requirements.

B. Alignment and Difficulty of the Proxy Task

The results of this study suggest that the difficulty level of a proxy task must be set appropriately for the task to be

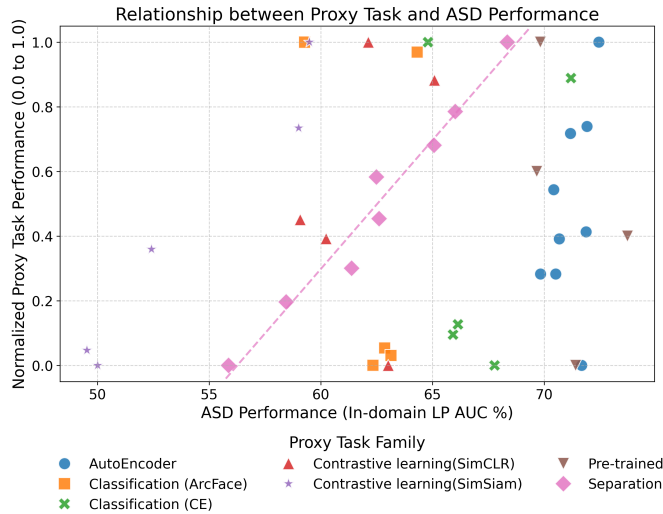


Fig. 2. Relationship between the proxy task and in-domain ASD performances. The normalized proxy task performance (y-axis) is plotted against in-domain LP AUC (%) (x-axis). The markers and colors denote the proxy task family. The dashed line indicates a linear trend for source separation, showing statistically significant correlation ($\rho = 0.98, p < 0.001$).

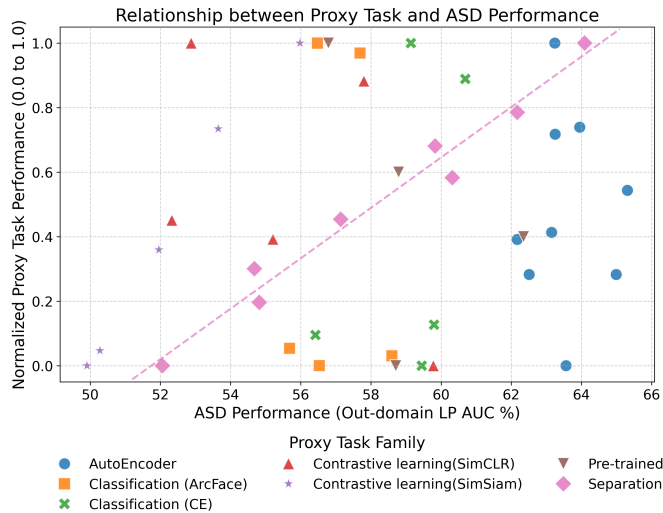


Fig. 3. Relationship between the proxy task and out-domain ASD performances. Normalized proxy task performance (y-axis) was plotted against out-domain LP AUC (%) (x-axis). The markers and colors denote the proxy task family. The dashed line indicates a linear trend for source separation ($\rho = 0.95, p < 0.01$).

effective, and the objective of this task must be well-aligned with the ASD goal.

The most distinct example is observed in the classification task. Across all experimental configurations, the proxy performance metric (F_1 -score) saturated above 97%, indicating a loss of discriminative power. Consequently, no statistical correlation with ASD performance was observed ($|\rho| \leq 0.3, p > 0.6$).

However, a different pattern emerged in the case of AE. Although AE performance steadily improved without reaching saturation ($MAE : 4.59 \rightarrow 4.13 \times 10^{-3}$), no significant correlation was found in the LP-based evaluation. A correlation appeared only in the MD evaluation ($\rho = -0.78, p = 0.018$),

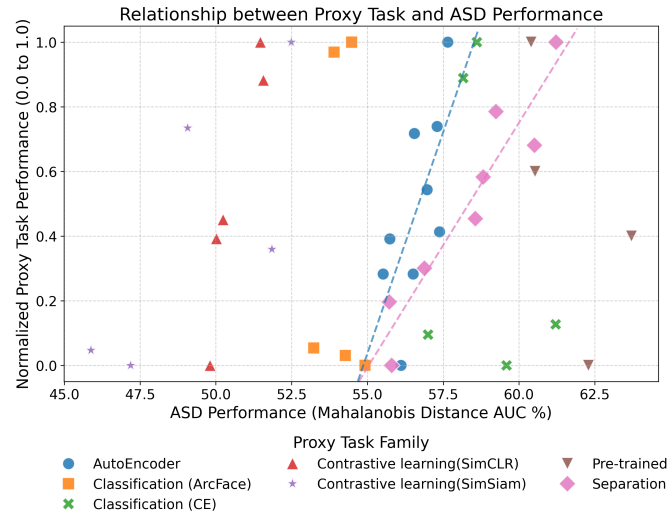


Fig. 4. Relationship between the proxy task performance and the ASD performance in terms of MD. Normalized proxy task performance (y-axis) is plotted against MD AUC (%) (x-axis). The markers and colors denote the proxy task family. The dashed lines indicate linear trends for statistically significant correlations: source separation ($\rho = 0.95, p < 0.001$) and AE ($\rho = -0.78, p < 0.05$).

indicating that the reconstruction objective was only partially aligned with the ASD task.

For contrastive learning, the training process fundamentally failed due to limitations in data quantity and diversity. Specifically, as the model capacity of SimSiam increased, the uniformity metric worsened (increased) from -0.82 to -0.18. This suggests a failure to acquire features suitable for ASD, yielding a marginal ASD performance of 52.49% based on the MD.

Conversely, source separation gradually improved in terms of the proxy metric (SI-SDRi: $2.29 \rightarrow 3.92$ dB), and a strong correlation with all ASD metrics was observed ($\rho > 0.950, p < 0.01$). This represents an ideal scenario in which appropriate task difficulty and objective alignment are satisfied. These findings highlight the necessity of carefully designing the difficulty of the proxy task and verifying its alignment with the target task during the design phase.

C. Characteristics of Learned Representations

Each proxy task induced distinct characteristics in the learned representation. Synthesizing the results from Tables II–VI reveals that the strengths of the acquired features vary considerably depending on the evaluation metric.

First, a trade-off was observed between linear separability and distributional compactness. The AE demonstrated superior performance in LP evaluations (in-domain 72.45%, out-domain 64.99%) but recorded relatively reduced MD performance (57.65%). Conversely, source separation, while achieving reduced LP scores (in-domain: 68.35%, out-domain: 64.09%), outperformed other proxy tasks in terms of the MD metric (61.22%). This suggests that depending on the training objective, the network prioritizes either establishing clear decision boundaries (separability) or minimizing the variance of normal data (compactness).

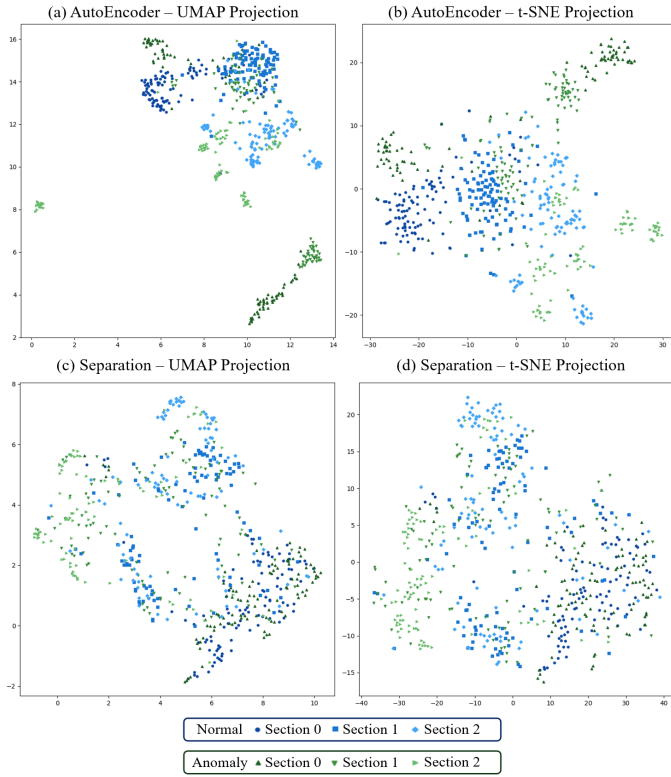


Fig. 5. Representations of the gearbox class from the trained AE (a)–(b) and separation (c)–(d) models, projected with UMAP and t-SNE. Projection results do not match quantitative MD AUC: 72.68% (separation) vs. 64.15% (AE).

Second, classification tasks yielded diverging characteristics based on model capacity. The smallest model, ResNet-18, excelled in linear separability but exhibited reduced compactness (in-domain LP: 71.20%, MD: 58.16%). In contrast, the most complex model, ResNet-152, exhibited superior compactness but degraded linear separability (in-domain LP: 66.14%, MD: 61.21%). Although pre-trained models achieved high in-domain performance, they exhibited the most performance reduction in out-domain settings, confirming a marked vulnerability to domain shifts (in-domain LP: 73.73% and out-domain LP: 62.35%).

Finally, we emphasize the limitations of evaluating ASD systems solely based on low-dimensional visualizations such as t-SNE or UMAP. Fig. 5 illustrates the projection results corresponding to the ‘gearbox’ class. The AE representations (Figs. 5(a)–(b)) appeared to clearly separate normal and anomalous samples; however, the actual quantitative AUC was only 64.15% with the MD. Alternatively, source separation representations (Figs. 5(c)–(d)) appeared less separated; however, they achieved a considerably increased AUC of 72.68% (an 8.5% margin). This discrepancy possibly arises because dimensionality reduction techniques prioritize preserving local neighborhood structures, potentially distorting the global high-dimensional characteristics relevant for anomaly detection. Therefore, qualitative visualization should always be complemented by diverse quantitative metrics for a reliable ASD evaluation.

D. Practical Implications

Synthesizing our experimental findings, we indicate that improvements in proxy task performance do not necessarily enhance ASD capabilities. In this section, we analyze the primary causes of this misalignment and propose a systematic verification protocol to address these issues.

First, balancing task difficulty and aligning objectives is critical. The task corresponding to classification was too trivial, saturating the performance but failing to provide discriminative representations. Conversely, contrastive learning tasks proved excessively difficult relative to the quantity and diversity of the dataset, causing model collapse and failure to learn meaningful features. The stable correlation observed with source separation may reflect the task, providing an appropriate level of difficulty for capturing the time-frequency structures of normal data. Therefore, designing a proxy task requires carefully tailoring the difficulty level to match the intrinsic characteristics of the dataset.

Second, multi-faceted metrics are required to evaluate the diverse properties of representations. The AE results imply that density estimation and boundary formation are distinct problems. Furthermore, even within the same proxy task, the characteristics of learned representations can shift depending on model capacity. For instance, in classification training, ResNet-18 excelled in LP tests, whereas ResNet-152 performed better in MD evaluations. This indicates that model complexity influences the formation of the feature space; therefore, this validates feature compactness and separability in a complementary manner.

Third, caution must be exercised when interpreting low-dimensional visualizations (e.g., t-SNE and UMAP). As discussed in Section VI-C, qualitative visualizations can be misleading; the AE appeared clearly separated despite poor quantitative performance, whereas source separation displayed the opposite trend. As dimensionality reduction techniques inherently distort global structures, relying solely on visualization for model selection is unreliable. Quantitative metrics must always accompany qualitative analysis.

Fourth, based on these analyses, we propose a three-stage alignment verification protocol. Future ASD research employing proxy tasks should extend beyond simple convergence checks and adopt the following systematic validation process:

- **Stage 1:** Verify the primary health of the proxy task training. Ensure that the proxy metric is neither excessively saturated (indicating a trivial task) nor indicative of training failure (indicating an overly complex task).
- **Stage 2:** Evaluate whether the learned representations are suitable for ASD. This involves assessing both linear separability and feature compactness or directly evaluating the features using an anomaly score calculator.
- **Stage 3:** Conduct a correlation analysis across various hyperparameter settings to definitively confirm that improvements in the proxy task align with actual gains in ASD performance.

By adopting this three-stage protocol, researchers can minimize trial-and-error and design highly effective proxy tasks for anomaly detection.

VII. CONCLUSION

This study systematically investigated the relationship between proxy task performance and ASD capability, an issue that has been largely overlooked in the existing literature despite having practical importance. Although proxy tasks are grounded in explicit assumptions (e.g., that anomalies increase reconstruction errors), the implicit premise that optimizing these proxy metrics directly improves detection performance had not been empirically verified. Therefore, we evaluated five proxy task configurations (AE, classification, source separation, contrastive learning, and pre-trained models) on the ToyADMOS and MIMII datasets via LP and MD analyses.

The experimental results indicate that the assumption that high proxy task performance guarantees high ASD performance does not generally apply. Only source separation demonstrated a strong positive correlation, i.e., improvements in SI-SDRi directly translated to ASD performance gains in LP and MD metrics. Conversely, classification failed to reveal a correlation due to performance saturation attributable to the trivial difficulty of the task, whereas contrastive learning showed no correlation owing to the limited acoustic diversity inherent in the dataset. The AE exhibited a correlation with distributional compactness (MD); however, no correlation was observed with linear separability (LP), suggesting that the optimal proxy task may vary depending on the evaluation metric.

The contributions of this study are threefold.

Firstly, this is the first study to quantitatively characterize the correlation between proxy tasks and ASD through extensive large-scale experiments.

Second, we propose a three-stage alignment verification protocol that comprehensively evaluates proxy performance and feature linear separability and distributional compactness.

Third, we empirically report various scenarios in which correlation breaks down, such as performance saturation, objective misalignment, and training failure, thereby highlighting the importance of appropriate difficulty and goal alignment for effective proxy task design.

However, the limitation of this study is that, as the experiments were limited to seven machine sound types, the generalizability to diverse acoustic environments was not fully verified.

Future research can analyze the complementary effects of multi-objective learning beyond single-task learning or develop adaptive proxy task selection methods that monitor task alignment during training. Furthermore, the impact of the architectural characteristics of the neural networks on proxy-target alignment can be analyzed.

In conclusion, this study proposes a new design paradigm that prioritizes the alignment between proxy tasks and ASD. We expect that the proposed three-stage alignment verification protocol will serve as a practical guideline for developing highly effective ASD systems.

REFERENCES

- [1] G. Valenzise, L. Gerosa, M. Tagliasacchi, F. Antonacci, and A. Sarti, “Scream and gunshot detection and localization for audio-surveillance systems,” in *2007 IEEE Conference on Advanced Video and Signal Based Surveillance*, 2007, pp. 21–26.
- [2] C. Clavel, L. Devillers, G. Richard, I. Vasilescu, and T. Ehretre, “Detection and analysis of abnormal situations through fear-type acoustic manifestations,” in *2007 IEEE International Conference on Acoustics, Speech and Signal Processing - ICASSP '07*, vol. 4, 2007, pp. IV-21–IV-24.
- [3] Y. Koizumi, S. Saito, H. Uematsu, Y. Kawachi, and N. Harada, “Unsupervised detection of anomalous sound based on deep learning and the neyman–pearson lemma,” *IEEE/ACM Transactions on Audio, Speech, and Language Processing*, vol. 27, no. 1, pp. 212–224, 2018.
- [4] A. K. Jardine, D. Lin, and D. Banjevic, “A review on machinery diagnostics and prognostics implementing condition-based maintenance,” *Mechanical Systems and Signal Processing*, vol. 20, no. 7, pp. 1483–1510, 2006.
- [5] Y. Koizumi, Y. Kawaguchi, K. Imoto, T. Nakamura, Y. Nikaido, R. Tanabe, H. Purohit, K. Suefusa, T. Endo, M. Yasuda, and N. Harada, “Description and discussion on DCASE2020 challenge task2: Unsupervised anomalous sound detection for machine condition monitoring,” in *Proceedings of the Detection and Classification of Acoustic Scenes and Events 2020 Workshop (DCASE2020)*, November 2020, pp. 81–85.
- [6] Y. Kawachi, Y. Koizumi, and N. Harada, “Complementary set variational autoencoder for supervised anomaly detection,” in *2018 IEEE International Conference on Acoustics, Speech and Signal Processing (ICASSP)*, 2018, pp. 2366–2370.
- [7] E. Marchi, F. Vesperini, F. Weninger, F. Eyben, S. Squartini, and B. Schuller, “Non-linear prediction with lstm recurrent neural networks for acoustic novelty detection,” in *2015 International Joint Conference on Neural Networks (IJCNN)*, 2015, pp. 1–7.
- [8] R. Giri, S. V. Tenneti, F. Cheng, K. Helwani, U. Isik, and A. Krishnaswamy, “Self-supervised classification for detecting anomalous sounds,” in *Proceedings of the Detection and Classification of Acoustic Scenes and Events 2020 Workshop (DCASE2020)*, Tokyo, Japan, November 2020, pp. 46–50.
- [9] H. Hojjati and N. Armanfard, “Self-supervised acoustic anomaly detection via contrastive learning,” in *ICASSP 2022 - 2022 IEEE International Conference on Acoustics, Speech and Signal Processing (ICASSP)*, 2022, pp. 3253–3257.
- [10] Y. Lee, J. Kim, and J. Ok, “Activity-guided industrial anomalous sound detection against interferences,” *arXiv preprint arXiv:2409.01885*, 2024.
- [11] A. A. T. Anvar and H. Mohammadi, “A novel application of deep transfer learning with audio pre-trained models in pump audio fault detection,” *Computers in Industry*, vol. 147, p. 103872, 2023.
- [12] E. Marchi, F. Vesperini, F. Eyben, S. Squartini, and B. Schuller, “A novel approach for automatic acoustic novelty detection using a denoising autoencoder with bidirectional lstm neural networks,” in *2015 IEEE International Conference on Acoustics, Speech and Signal Processing (ICASSP)*, 2015, pp. 1996–2000.
- [13] J. Deng, J. Guo, N. Xue, and S. Zafeiriou, “Arcface: Additive angular margin loss for deep face recognition,” in *2019 IEEE/CVF Conference on Computer Vision and Pattern Recognition (CVPR)*, 2019, pp. 4685–4694.
- [14] A. Kolesnikov, X. Zhai, and L. Beyer, “Revisiting self-supervised visual representation learning,” in *Proceedings of the IEEE/CVF conference on computer vision and pattern recognition*, 2019, pp. 1920–1929.
- [15] K. Lee, K. Lee, H. Lee, and J. Shin, “A simple unified framework for detecting out-of-distribution samples and adversarial attacks,” *Advances in neural information processing systems*, vol. 31, 2018.
- [16] C. Clavel, T. Ehretre, and G. Richard, “Events detection for an audio-based surveillance system,” in *2005 IEEE International Conference on Multimedia and Expo*, 2005, pp. 1306–1309.
- [17] P. Foggia, N. Petkov, A. Saggesse, N. Strisciuglio, and M. Vento, “Audio surveillance of roads: A system for detecting anomalous sounds,” *IEEE Transactions on Intelligent Transportation Systems*, vol. 17, no. 1, pp. 279–288, 2016.
- [18] J. Rubin, R. Abreu, A. Ganguli, S. Nelaturi, I. Matei, and K. Sricharan, “Recognizing abnormal heart sounds using deep learning,” *arXiv preprint arXiv:1707.04642*, 2017.
- [19] J. Lee, H. Choi, D. Park, Y. Chung, H.-Y. Kim, and S. Yoon, “Fault detection and diagnosis of railway point machines by sound analysis,” *Sensors*, vol. 16, no. 4, 2016.
- [20] D. Park, Y. Hoshi, and C. C. Kemp, “A multimodal anomaly detector for robot-assisted feeding using an lstm-based variational autoencoder,” *IEEE Robotics and Automation Letters*, vol. 3, no. 3, pp. 1544–1551, 2018.
- [21] Y. Koizumi, S. Saito, H. Uematsu, N. Harada, and K. Imoto, “ToyADMOS: A dataset of miniature-machine operating sounds for anomalous sound detection,” in *2019 IEEE Workshop on Applications of Signal*

Processing to Audio and Acoustics (WASPAA). IEEE, 2019, pp. 313–317.

[22] H. Purohit, R. Tanabe, K. Ichige, T. Endo, Y. Nikaido, K. Suefusa, and Y. Kawaguchi, “MIMII dataset: Sound dataset for malfunctioning industrial machine investigation and inspection,” in *Proc. Detection and Classification of Acoustic Scenes and Events 2019 Workshop (DCASE2019)*, New York, NY, USA, Oct. 2019, pp. 161–165.

[23] N. Harada, D. Niizumi, D. Takeuchi, Y. Ohishi, M. Yasuda, and S. Saito, “Toyadmos2: Another dataset of miniature-machine operating sounds for anomalous sound detection under domain shift conditions,” in *Proceedings of the 6th Detection and Classification of Acoustic Scenes and Events 2021 Workshop (DCASE2021)*, Barcelona, Spain, November 2021, pp. 1–5.

[24] K. Dohi, K. Imoto, N. Harada, D. Niizumi, Y. Koizumi, T. Nishida, H. Purohit, R. Tanabe, T. Endo, M. Yamamoto, and Y. Kawaguchi, “Description and discussion on DCASE 2022 challenge task 2: Unsupervised anomalous sound detection for machine condition monitoring applying domain generalization techniques,” in *Proceedings of the 7th Detection and Classification of Acoustic Scenes and Events 2022 Workshop (DCASE2022)*, Nancy, France, November 2022, pp. 1–5.

[25] J. Guan, Y. Liu, Q. Kong, F. Xiao, Q. Zhu, J. Tian, and W. Wang, “Transformer-based autoencoder with id constraint for unsupervised anomalous sound detection,” *EURASIP journal on audio, speech, and music processing*, vol. 2023, no. 1, p. 42, 2023.

[26] I. Kuroyanagi, T. Hayashi, Y. Adachi, T. Yoshimura, K. Takeda, and T. Toda, “Anomalous sound detection with ensemble of autoencoder and binary classification approaches,” *DCASE2021 Challenge*, 2021.

[27] S. Shin and S. Lee, “Representational learning for an anomalous sound detection system with source separation model,” in *Proceedings of the Detection and Classification of Acoustic Scenes and Events 2024 Workshop (DCASE2024)*, Tokyo, Japan, October 2024, pp. 146–150.

[28] J. Wu, F. Yang, and W. Hu, “Unsupervised anomalous sound detection for industrial monitoring based on arcface classifier and gaussian mixture model,” *Applied Acoustics*, vol. 203, p. 109188, 2023.

[29] K. Wilkinghoff and F. Kurth, “Why do angular margin losses work well for semi-supervised anomalous sound detection?” *IEEE/ACM Transactions on Audio, Speech, and Language Processing*, vol. 32, pp. 608–622, 2023.

[30] T. Chen, S. Kornblith, M. Norouzi, and G. Hinton, “A simple framework for contrastive learning of visual representations,” in *International conference on machine learning*. PMLR, 2020, pp. 1597–1607.

[31] X. Chen and K. He, “Exploring simple siamese representation learning,” in *Proceedings of the IEEE/CVF conference on computer vision and pattern recognition*, 2021, pp. 15750–15758.

[32] J. Guan, F. Xiao, Y. Liu, Q. Zhu, and W. Wang, “Anomalous sound detection using audio representation with machine id based contrastive learning pretraining,” in *ICASSP 2023-2023 IEEE International Conference on Acoustics, Speech and Signal Processing (ICASSP)*. IEEE, 2023, pp. 1–5.

[33] S. Chen, Y. Wu, C. Wang, S. Liu, D. Tompkins, Z. Chen, and F. Wei, “Beats: Audio pre-training with acoustic tokenizers,” *arXiv preprint arXiv:2212.09058*, 2022.

[34] W. Chen, Y. Liang, Z. Ma, Z. Zheng, and X. Chen, “Eat: Self-supervised pre-training with efficient audio transformer,” *arXiv preprint arXiv:2401.03497*, 2024.

[35] L. Wang, “Pre-trained model enhanced anomalous sound detection system for dcase2025 task2,” *DCASE2025 Challenge*, Tech. Rep., June 2025.

[36] P. Saengthong and T. Shinozaki, “Genrep for first-shot unsupervised anomalous sound detection of dcase 2025 challenge,” *DCASE2025 Challenge*, Tech. Rep., June 2025.

[37] L. v. d. Maaten and G. Hinton, “Visualizing data using t-sne,” *Journal of machine learning research*, vol. 9, no. Nov, pp. 2579–2605, 2008.

[38] L. McInnes, J. Healy, and J. Melville, “Umap: Uniform manifold approximation and projection for dimension reduction,” *arXiv preprint arXiv:1802.03426*, 2018.

[39] G. Alain and Y. Bengio, “Understanding intermediate layers using linear classifier probes,” *arXiv preprint arXiv:1610.01644*, 2016.

[40] J. Hewitt and P. Liang, “Designing and interpreting probes with control tasks,” *arXiv preprint arXiv:1909.03368*, 2019.

[41] T. Wang and P. Isola, “Understanding contrastive representation learning through alignment and uniformity on the hypersphere,” in *International conference on machine learning*. PMLR, 2020, pp. 9929–9939.

[42] L. Ericsson, H. Gouk, and T. M. Hospedales, “How well do self-supervised models transfer?” in *Proceedings of the IEEE/CVF conference on computer vision and pattern recognition*, 2021, pp. 5414–5423.

[43] I. Loshchilov and F. Hutter, “Decoupled weight decay regularization,” *arXiv preprint arXiv:1711.05101*, 2017.

[44] K. He, X. Zhang, S. Ren, and J. Sun, “Deep residual learning for image recognition,” in *Proceedings of the IEEE conference on computer vision and pattern recognition*, 2016, pp. 770–778.

[45] K. Shimonishi, K. Dohi, and Y. Kawaguchi, “Anomalous sound detection based on sound separation,” *INTERSPEECH 2023*, 2023.

[46] S. Abdulatif, R. Cao, and B. Yang, “Cmgan: Conformer-based metric-gan for monaural speech enhancement,” *IEEE/ACM Transactions on Audio, Speech, and Language Processing*, vol. 32, pp. 2477–2493, 2024.

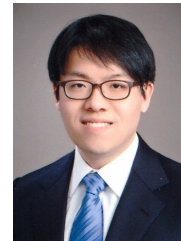
[47] A. Gulati, J. Qin, C.-C. Chiu, N. Parmar, Y. Zhang, J. Yu, W. Han, S. Wang, Z. Zhang, Y. Wu *et al.*, “Conformer: Convolution-augmented transformer for speech recognition,” in *Proc. Interspeech 2020*, 2020, pp. 5036–5040.

[48] J. F. Gemmeke, D. P. Ellis, D. Freedman, A. Jansen, W. Lawrence, R. C. Moore, M. Plakal, and M. Ritter, “Audio set: An ontology and human-labeled dataset for audio events,” in *2017 IEEE international conference on acoustics, speech and signal processing (ICASSP)*. IEEE, 2017, pp. 776–780.

[49] J. Le Roux, S. Wisdom, H. Erdogan, and J. R. Hershey, “Sdr-half-baked or well done?” in *ICASSP 2019-2019 IEEE International Conference on Acoustics, Speech and Signal Processing (ICASSP)*. IEEE, 2019, pp. 626–630.



SEUNGHYEON SHIN received the B.S. degree in mechanical engineering from Dong-A University, Busan, in 2020, and the M.S. degree in electronic engineering from Kyungpook National University, Daegu, in 2022. He is currently a Ph.D. student at Kyungpook National University. His research interests include acoustic anomaly detection, acoustic source separation and acoustic signal processing.



SEOKJIN LEE (Member, IEEE) received the B.S., M.S., and Ph.D. degrees in electrical and computer engineering from Seoul National University, in 2006, 2008, and 2012, respectively. From 2012 to 2014, he was a Senior Research Engineer at LG Electronics. From 2014 to 2018, he was an Assistant Professor at the Department of Electronics Engineering, Kyonggi University, Suwon, Republic of Korea. Since 2018, he has been an Assistant Professor (promoted to an Professor, in 2025) with the School of Electrical and Electronics Engineering, Kyungpook National University, Daegu, Republic of Korea. His research interests include acoustic, sound and music signal processing, array signal processing, and blind source separation.